Simultaneous Tuning of Static Synchronous Series Compensator and Multi-Band Power System Stabilizers to Mitigate Sub-Synchronous Resonances in Power Systems

Majid Moazzami[1,2*], Hassan Fayazi[1,2], Bahador Fani[1,2], Shadi Jalali[1,2], Ghazanfar Shahgholian[1,2]
1-Smart Microgrid Research Center, Najafabad Branch, Islamic Azad University, Najafabad, Iran.
Email: m_moazzami@pel.iaun.ac.ir(Corresponding Author)
2-Department of Electrical Engineering, Najafabad Branch, Islamic Azad University, Najafabad, Iran.
Emails: hasanfayazi@sel.iaun.ac.ir, bahador.fani@gmail.com, shadi_power39@yahoo.com, shahgholian@iaun.ac.ir

Received: December 2018 Revised: April 2019 Accepted: May 2019

ABSTRACT:
In this paper, the concept of simultaneous tuning of static synchronous series compensators and multi-band power system stabilizers for damping out sub-synchronous resonances in a series compensated power system is presented. To achieve an effective damping effect, a supplementary sub-synchronous damping controller is added to the static synchronous series compensator. The teaching-learning-based optimization algorithm is employed for the simultaneous adjustment of the parameters of both the supplementary sub-synchronous damping controller and the power system stabilizer. The proposed method is executed on the IEEE Benchmark system and simulation results are provided to verify its capability in removing sub-synchronous resonances and maintaining the stability of the underlying system.

KEYWORDS: Sub-Synchronous Resonances, Static Synchronous Series Compensators, Teaching-Learning-Based Optimization Algorithm; Power System Stabilizer.

1. INTRODUCTION

Series compensation with capacitor is a conventional method used to reduce the problems caused by the reactance of transmission lines. It has such advantages as temporarily improved line stability, enhanced transmission line capacity, adjusted load between series lines, and improvement power coefficient as well as reduced voltage losses, changes in abrupt voltage resonance and power loss. Despite these benefits, series capacitors might increase the risk of interactions/interferences between the electrical power system and the turbine generator's rotor torsional modes. This phenomenon is known as sub-synchronous resonance or SSR for short [1]. These resonances damage the turbo-generator shaft, reduce their life time, and lead to instability in the rated sub-frequency of the system. Hence, their application in power networks must be based on thorough evaluations of the SSR while proper strategies, basically including Flexible Alternating Current Transmission System (FACTS) devices and power system stabilizers (PSS), also need to be provisioned in order to reduce their side effects.

Flexible Alternating Current Transmission System (FACTS) devices are considered to be powerful tools in controlling the active power and voltage in power systems. In [2], a PI controller is designed to reduce the SSR effects for unified power flow controllers (UPFC). In [3], the SSR phenomenon is studied through the improved model of static Var compensators. In [4], omission of the SSR is studied via changing the control method in gate-controlled series capacitors (GCSC). In [5], Static Synchronous Compensators (STATCOM) are designed and functionally analyzed in an attempt to remove SSR effects. Controlling the branches originating from the SSR is accomplished by applying thyristor-controlled series compensators (TCSC) in [6]. The Thyristor Controlled Series Compensation (TCSC) fire angel is set in [7] to reduce the SSR effects using an adaptive neural controller. In order to improve upon the system's function against SSR, a multi-purpose evolutionary optimization algorithm is used in [8] to determine the parameters of the static synchronous series compensator (SSSC). In order to prevent the torsion resonances in series compensated transmission lines, an SSSC with a fixed capacitor is proposed in [9]. Two novel methods are proposed in [10] to control the SSSC for series dynamic compensation and voltage setting. Finally, in [11], SSSC parameters are adjusted using the fuzzy logic for system resonance damping.

Different controlling methods of PSS design have been proposed, among which the classic power system stabilizers (CPSS) have attracted a lot attention among researchers due to their structural simplicity, great flexibility, and ease of implementation. In [12], PSS parameters are adjusted using an adjusted genetic algorithm. In [13], fuzzy PID controllers are used and their parameters are determined using particle swarm optimization (PSO) algorithm. The great need for damping a large spectrum of global, inter-area, and local electromechanical resonances has led to the development of the multi-band power system stabilizer concept. In the configuration of multi-band stabilizers, three separate bands are applied to dampen low, medium, and high frequencies. In [14], a multi-band stabilizer is designed using a culture-PSO-Co evolutionary (CPCE) algorithm for a multi-machine system.

This paper proposed the simultaneous setting and application of an SSSC equipped with an auxiliary supplementary sub-synchronous damping controller (SSDC) and an MB-PSS for damping SSR. For efficient damping, a teaching-learning-based optimization (TLBO) algorithm is used to adjust the SSD and MB-PSS parameters. Simulation results show the effectiveness of the proposed approach for damping SSR in power systems.

In the second part of the paper, SSSC and the control structure is initially described and detailed. This is followed by a description of the classic and multi-band power system stabilizers. Then, the problem is formulated with regard to the SSSC, PSS, and TLBO optimization algorithm and its implementation is introduced. Section 3 presents the test system studied while Section 4 presents the simulation results. Finally, conclusions are presented in Section 5.

2. THE PROPOSED METHOD

2.1. Static Synchronous Series Compensator (SSSC)

SSSC voltage source, which is a DC type, is connected to the transmission network through an inverter. Based on the switching style and angle, the inverter converts the DC voltage to the AC before injecting the current into the network [15]. The SSSC is capable of efficiently controlling the flow power due to its bimodal functioning both as a reactor and a capacitor.

2.1.1. Control structure of the SSSC

SSSCs come with an intrinsic damping ability although this ability may not be adequate for certain applications. Accordingly, a supplementary sub-synchronous damping controller (SSDC) should be designed and added to the SSSC to ensure efficient damping [16]. Fig. 1 shows the control structure of the load transmission by applying an SSDC in an SSSC. In this configuration, two basic controllers are implemented in the SSSC: 1) the V_q voltage, and 2) the DC voltage regulator. The main strategy adopted to control the SSSC for damping SSR resonances involves the application of basic stabilizing signals. Generator rotor speed deviation, $\Delta\omega$, includes components of all the torsional modes. Thus, if the rotor speed deviation is used to control the SSSC, all the torsional modes will be influenced in addition to the one related to the generator mass. As shown in Fig. 1, the input of the selected SSDC is the generator rotor speed deviation. After passing through a washout filter, the input excites the K_d derivative gain. The output signal of the derivative gain represents the presence of SSR in the power system. Accordingly, the SSDC uses the rotor speed for modulating the V_q injected voltage in order to yield improved damping of instable torsional modes. In Fig. 1, V_{qref} represents the optimum reference injected voltage in the load transmission control loop in the steady state.

In the block diagram of Fig. 1, V_{d_conv} and V_{q_conv} define the convertor voltage elements (V_{conv}), which have the same phase as the current and vertical to it. The control system includes the following elements:

- A phase locked loop (PLL) synchronizes the current of I with positive sequence elements. PLL output (with an angle of θ=ωt) is applied to measure the voltage components along the horizontal and vertical axes as well as the AC three-phase currents (Vd, Vq or Id, Iq depicted in Fig. 1).

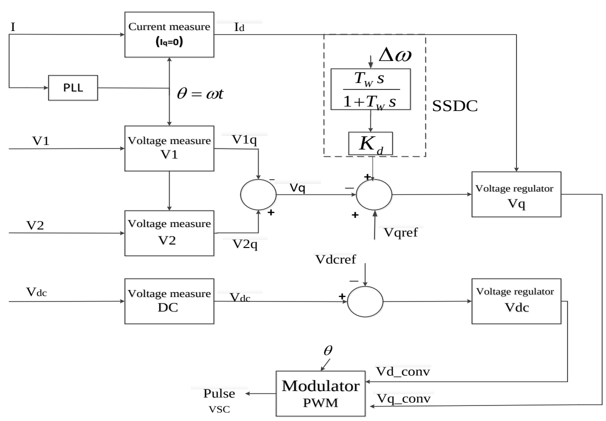

Fig. 1. SSSC load transmission control structure with a SSDC

- Measuring systems are used to measure the positive sequence q components of V1 and V2 voltages (V2q and V1q) as well as those of V_{dc}.
- The AC and DC voltage regulators measure the two voltage converter components of V_{d_conv} and V_{q_conv}, which are necessary to ensure optimum DC (V_{dcref}) and injected (V_{qref}) voltages. V_q voltage regulator is supported by a lead regulator which forecasts the

V_{conv} voltage (i.e., the injected voltage on the side of the VSC transformer) by measuring the Id current.

The transformation function of the SSDC is given in (1).

$$y = \frac{T_W s}{1+T_W s} \Delta\omega K_d s \quad (1)$$

In a SSDC, the washout block function is a high pass filter with a time constant of T_W that suffices to pass the signals related to oscillations in the input signal without any alteration.

In order to have an optimum damping, the K_d derivative gain should be determined. In the steady state conditions, the outputs of both the SSDC and V_{qref} are constant values.

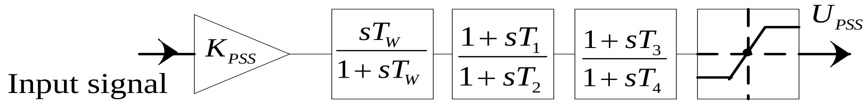

Fig. 2. The structure of a CPSS stabilizer.

2.2. Power System Stabilizer

2.2.1. Classic power system stabilizer (CPSS)

The structure of a CPSS is depicted in Fig. 2. In this stabilizer, either the speed signal or the difference between the mechanical and electrical powers is used as the input signal. This structure is composed of a washout block and a compensator. The output signal of the compensator is employed as the supplement input to the excitation system. A T_w time constant of 10s is assumed. K_{PSS} is the gain while and T_1 and T_2 are the time constants of the two-level lead and lag compensators. Here, the coefficients of T_1-T_4 and the stabilizer gain are adjusted by the TLBO algorithm.

2.2.2. MB-PSS power system stabilizer

The structure of the IEEE 4B multi-band stabilizer is introduced and described in [17]. Any of the three given bands are composed of a differential band pass filter, a gain, and a limiter. The output stabilizer signal is generated by combining the outputs from the three bands mentioned after they are passed through the final limiter. The resulting signal is finally integrated into the generator voltage set point to improve upon the damping of electromechanical resonances. The IEEE 4B MB-PSS block diagram and basic concept of three band PSS are shown in Figs. 3(a) and 3 (b) respectively. As explained earlier, the TLBO algorithm is used to configure and adjust MB-PSS parameters. In this process, the computation cost can be reduced by taking advantage of the structure in Fig. 3 (a), in which the parameters *T2*, *T4*, *T6*, and *T8* for all three bands are set to 0.01. The MB-PSS, therefore, requires 21 parameters to be adjusted. These parameters also include the frequencies of *FH*, *FI*, and *FL* as well as the gain parameters of *KH*, *KI*, and *KL*.

2.3. Optimization Problem

In the proposed method, the SSDC and PSS are configured in such a way that they minimize the mode resonances and dampen the SSR. Thus, the *f* function may be formulated as in (2) below:

$$f = \int_{t=0}^{t=t_{sim}} t\,|\Delta\omega|\,dt \quad (2)$$

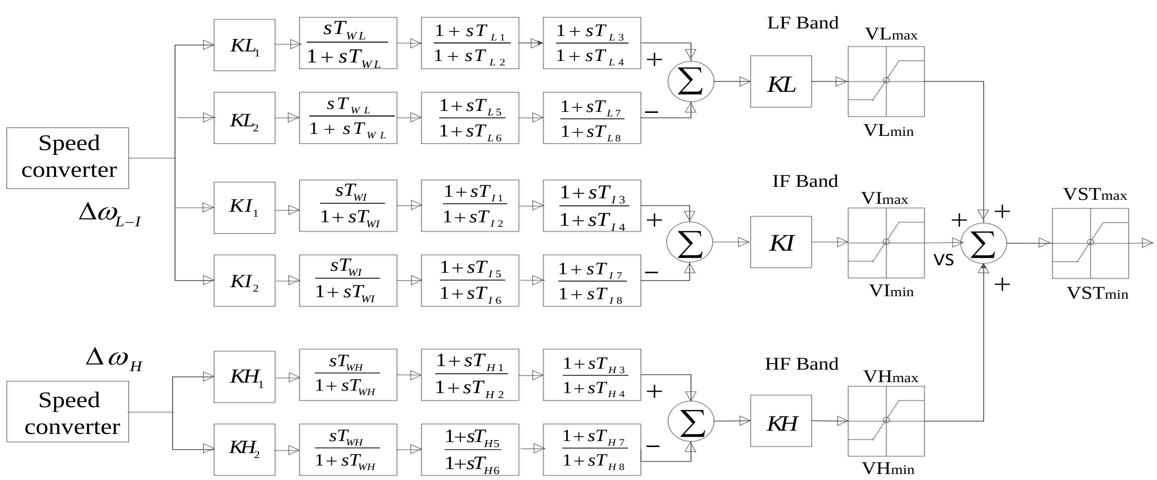

(a)

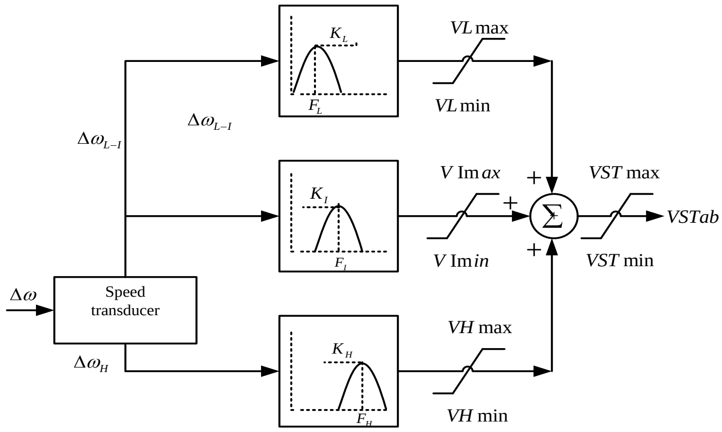

(b)

Fig. 3. (a): Block diagram of the MB-PSS IEEE 4B, (b): Basic concept of three band PSS [14] and [17].

Where, t_{sim} represents the simulation time and $\Delta\omega$ is the rotor speed. The design problem can be formulated as a constrained optimization problem expressed by (3), in which, the high and low limits of the SSDC parameter and the stabilizer are represented by the power MB-PSS and CPSS.

$$\begin{cases} \min f \\ s.t \\ K_{d\min} \le K_d \le K_{d\max} \qquad SSDC\ parameter \\ \left. \begin{array}{l} K_{i\min} \le K_{iPSS} \le K_{i\max} \\ T_{j\min} \le T_{jPSS} \le T_{j\max} \end{array} \right\} \ PSS\ parameters \end{cases} \tag{3}$$

2.3.1. TLBO optimization algorithm

The TLBO population-based optimization algorithm has been used to model teacher impact on learners. It is essentially a learning algorithm based on the influence of a teacher's instruction on the learners' learning in a classroom setting. Teachers and learners are the two main components of the algorithm describing the two basic modes of education, that imparted by the teacher (the teacher-phase) and the interactions among learners (the learning phase). The output of the TLBO algorithm in terms of results or student scores depends on the quality of teachers. Teachers are usually aware of the fact that as individuals they can improve the education process so that learners gain better results. In addition, learners interact with their peers to improve their learning toward better results.

In a classroom setting where an instructor teaches his/her students, if the students' learning is evaluated after the teaching is accomplished by the instructor, the learning achieved by the learners can be expressed by a normal function. In this distribution, the learning level is compared with the instructor's teaching. The instructor in this situation is the omniscient member of the present community who is considered to be the best learner. He/she tries his/her best to elevate the average knowledge and competence of his/her learners.

The instructor's teaching quality and the learners' participation and interactions in this learning environment are the decisive factors that determine the average level of learning achieved. A number of methods may be solicited to improve learner learning and knowledge level; these may be classified in two major categories. The first one involves the instructor's knowledge and expertise that might be enhanced through further in-service training. The second one concerns the learners who can improve their learning by cooperation and interaction with each other.

Based on the above teaching-learning process, a mathematical average is provided and expanded to optimize a continuous non-linear function. This then comprises the TLBO optimization method.

The TLBO process comprises the two aspects called the teacher's phase and the learner's phase as described below.

a) The teacher's phase: This phase of the algorithm simulates the learning of the students (or learners) as a result of the teacher's instruction. During this phase, a teacher shares knowledge with the learners and does every effort to augment the mean score (achievement) of the class.

Teacher is considered the most knowledgeable person, or the omniscient member, in the class. He/she imparts knowledge to learners in order to elevate their knowledge level and improve the learning efficiency realized in class average scores.

Although the teacher expectedly exercises maximum efforts to increase the knowledge level of the whole class, learners will only gain knowledge in proportion to the teaching quality and his/her learning quality. If *Mi* and *Ti* are taken to be average grades and the teacher is one and the same person, *Ti* is trying to get *Mi* to bolster their level. Thus, the teacher phase may be formulated as follows:

$$DM_i = rand_i \times (T_i - T_F M_i)$$
$$T_F = round(1 + rand(0,1)) \quad (4)$$
$$X_i^{new} = X_i^{old} + DM_i$$

Where, $rand_i$ is a random number between [0,1]. T_F is the teacher who decides about the average modified. The new value of X_i is accepted when the value of fitness is better than that of the previous function [18]. The average score of a class depends on the teacher's teaching quality. However, this average can be raised to a reasonable level depending on the capabilities of the learners in the class.

b) The learner's phase: This phase of the algorithm simulates learning by the learners through interactions among themselves. Learner A will gain new information from learner B if there is an information gap between the two; in other words, if learner B possesses more knowledge and is more competent than learner A. Learning in this phase is expressed as follows:

1. *Xi* and *Xj* are randomly chosen ($i \neq$ j).

2. Based on the fitness function, if $F(Xi) < F(Xj)$, the new inclusive is $X_i^{new} = rand_i \times (X_i - X_j)$.

3. A replacement can be performed if the new value of *Xi* is better than its previous value [18].

Learners can exploit either of two different ways, or both, to increase their knowledge. One is to use the instructor's teaching and the other is interactions with other learners, which can take the different forms of group work, lectures, etc. If there is a more competent learner, the others can get help or advice to enhance their knowledge.

2.3.2. Applying the TLBO method to optimization problems

Below is a step-by-step procedure for implementing the TLBO method [19]:

Step 1: Define the optimization problem and assign initial values to parameters;

Step 2: Determine the values for the population representing the number of learners;

Step 3: Select the best solution as the instructor;

Step 4 (learner phase): Learners enhance their knowledge through bilateral or multilateral interactions; and

Step 5 (Defining the end criterion): If maximum learning is achieved, then the task is completed. Otherwise, go back to Step 3;

In this method, the following three rules are observed in select the best solution:

1) If there are two practical and impractical solutions, then the practical one is selected;

2) If the two solutions are practical, then the one with a better objective function is selected; and

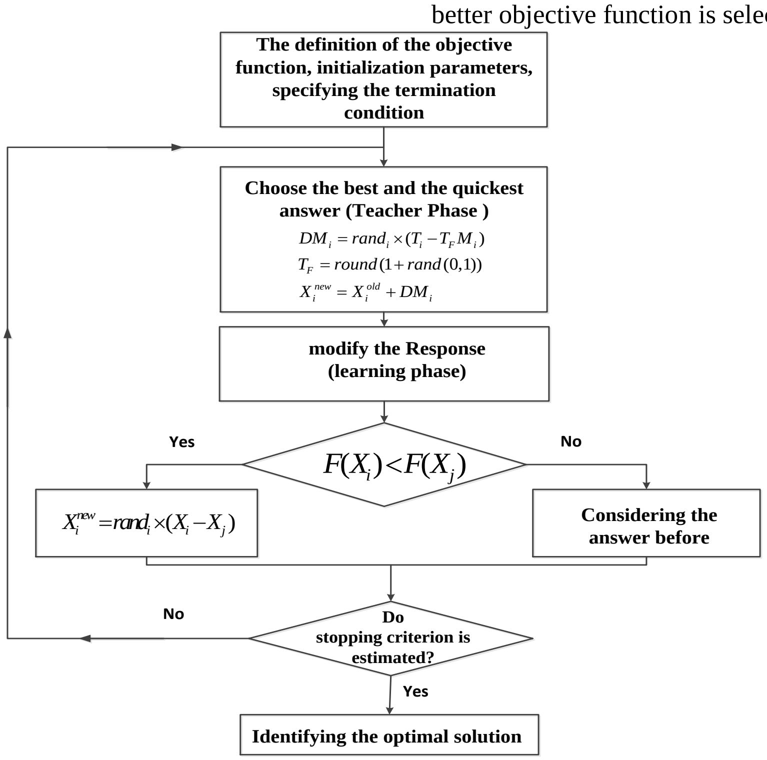

Fig. 4. TLBO optimization algorithm flowchart.

3) If the two solutions are impractical, the one is selected which imposes the least limitation.

These rules are utilized at the end of the learner and instructor phases to select the final solution. In this paper, the TLBO algorithm is employed to solve the proposed optimization problem and to determine the optimum parameters. The steps for implementing the TLBO algorithm are summarized in Fig. 4.

3. UNDER STUDY TEST SYSTEM

The IEEE benchmark system shown in Fig. 5 was considered to evaluate the capabilities of the proposed method for damping sub-synchronous resonances. In this model, a generator is connected to an infinite bus through two series capacitors, one of which includes a compensative series capacitor.

The system is designed to study the negative damping generated due to self-triggering. It is a practical model as it best resembles the real operational conditions of a power system [20]. As shown in Fig. 6, the SSSC injects a voltage in series to the transmission line.

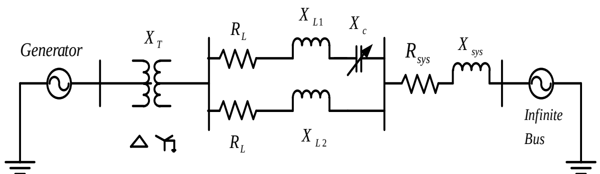

Fig. 5. IEEE benchmark system for SSR study [21].

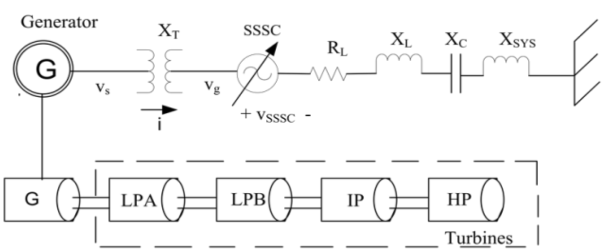

Fig. 6. IEEE initial criteria model with SSSC.

4. SIMULATION RESULTS

Parameter optimization and simulations are performed based on the initial operating conditions and the following assumptions:

a) The generator delivers 1-per-unit power to the transmission line and the values of the generator voltage and infinite bus are adjusted accordingly (1-per-unit);

b) The compensation level provided through the series capacitor is adjusted at 55%; and

c) It is assumed that the three-phase to the ground fault occurs at the beginning of line 2 at t=0 before it is removed at t=1.

In the simulation procedure, 2000 and 500 iterations are considered for the general and local queries respectively, in the TLBO method to ensure desirable operation. It is worth noting that several runs of the TLBO algorithm are performed. Optimum parameters are selected for the SSDC, CPSS, and MB-PSS based on the average values. The values for all the parameter are reported in Tables 1 through 4. To show the operational accuracy of the proposed algorithm, these values were also determined by the chaotic optimization algorithm (COA) [22] as provided in these same Tables.

Two SSR generation scenarios are employed to verify the efficiency of the proposed method and SSR removal strategies are simulated under the following four conditions using the relevant software:

a) In the presence of SSSC only;

b) In the presence of both SSSC and CPSS with the power input for CPSS;

c) In the presence of both SSSC and CPSS with the speed input for CPSS; and

d) In the presence of both SSSC and MB-PSS (the proposed method).

4.1. SSR Scenarios

4.1.1. Scenario 1:

In this scenario, the torque applied to the generator is reduced by 10% at t=5s and it is restored to its initial state at t=1s. In this case, the series compensation level is 55% and the working conditions are P=0.85 pu and V_t=1 pu. If the SSSC block is not present, the power system will suffer SSRs and subsequently becomes instable. Fig. 7 shows changes in the rotor angular velocity due to minor resonances. The simulation results for each of the SSR omission strategies are shown in Figs. 8 and 9.

4.1.2. Scenario 2:

According to this scenario, transmission line 2 is disconnected at t=1s and reconnected at t=4s. The variations in rotor angular velocity caused by this disturbance are shown in Fig. 10 and the simulation results for each of the SSR omission strategies are illustrated in Figs. 11 and 12.

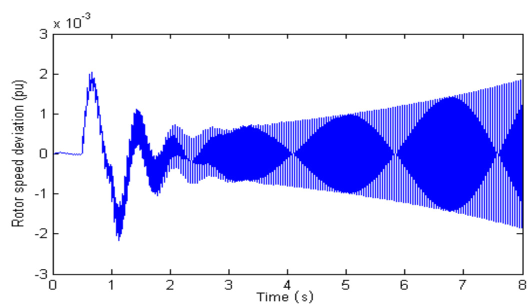

Fig. 7. Variations in rotor angular velocity in the 1st SSR scenario.

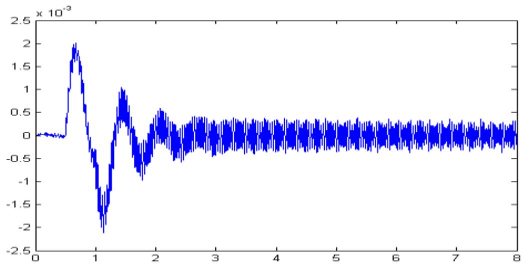

Fig. 8. Variations in rotor angular velocity in the 1st SSR scenario with SSSC.

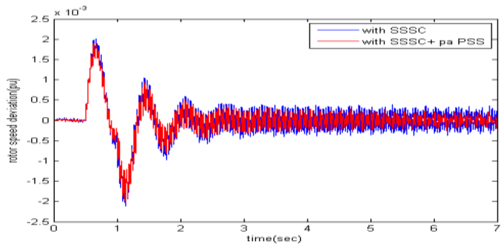

(a)

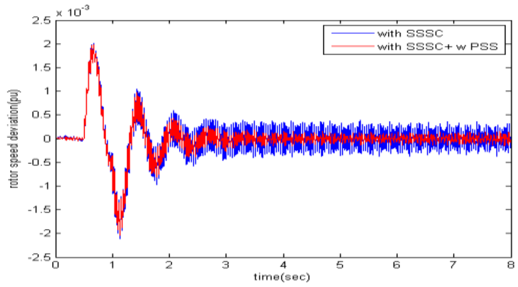

(b)

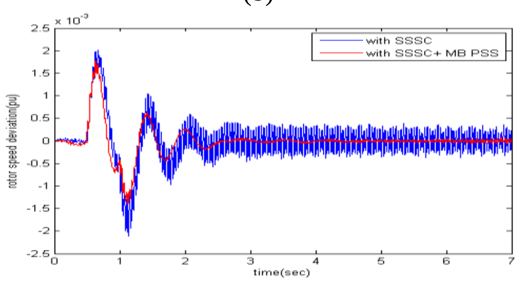

(c)

Fig. 9. Variations in rotor angular velocity in the 1st SSR scenario: a) with SSSC and CPSS with the power input, b) with SSSC and CPSS with speed input, and c) with SSSC and MB- PSS.

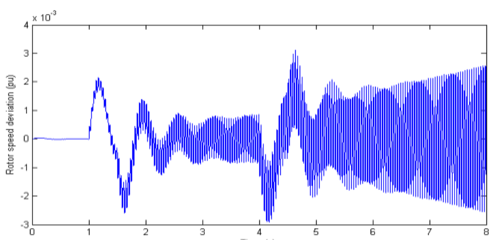

Fig. 10. Variations in rotor angular velocity in the 2nd SSR scenario.

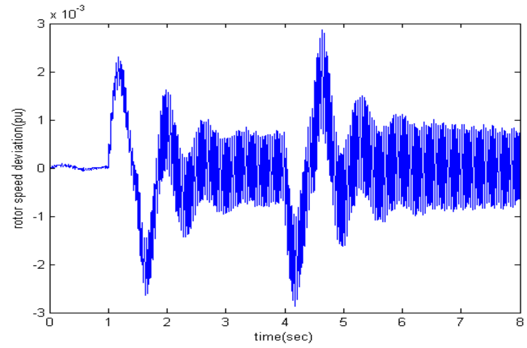

Fig. 11. Variations in rotor angular velocity in the 2st SSR scenario with SSSC.

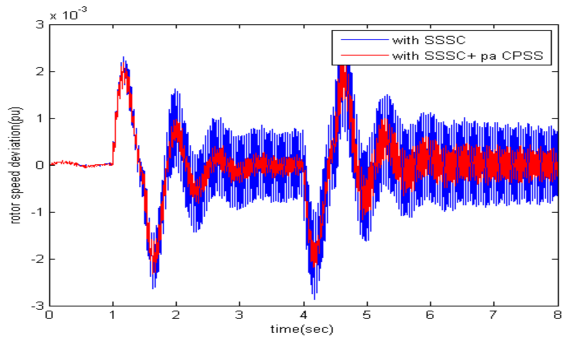

(a)

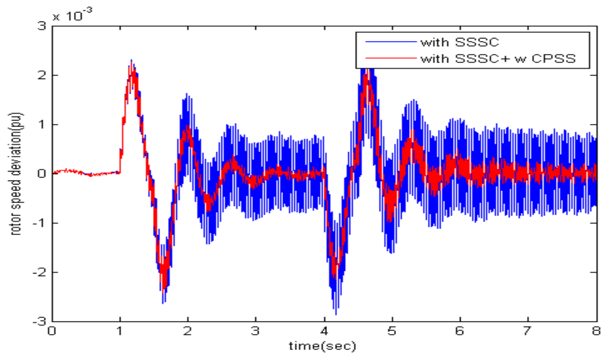

(b)

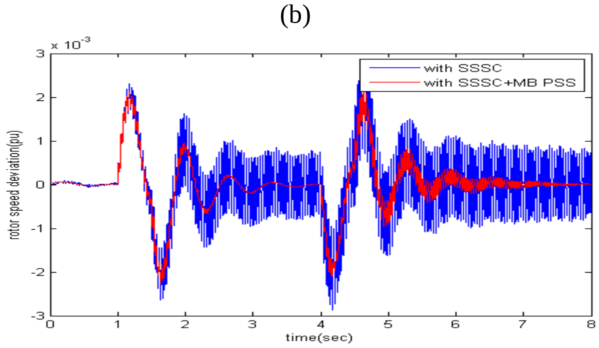

(c)

Fig. 12. Variations in rotor angular velocity in the 2nd SSR scenario: a) with SSSC and CPSS with the power input, b) with SSSC and CPSS with speed input, and c) with SSSC and MB-PSS.

Table 1. MB-PSS parameter setting.

	T1	T3	T5	T7	K1	K2	K
The high-pass of COA Method	0.011	0.005	0.834	0.010	1.000	1.000	1.000
The high-pass of TLBO Method	0.0105	0.0046	0.846	0.0102	1.005	1.004	1.006
The band pass of COA Method	0.005	0.010	0.657	0.010	1.500	2.320	2.720
The band pass of TLBO Method	0.0046	0.0102	0.668	0.0102	1.495	2.342	2.680
Method The low-pass of COA	0.591	0.010	0.005	0.010	9.400	1.170	3.180
Method The low-pass of TLBO	0.583	0.0102	0.0046	0.0102	9.456	1.176	3.201

Table 2. CPSS parameter setting with speed input.

	T_1	T_2	T_3	T_4	K_{PSS}
COA Method	0.005	0.002	3.000	5.4000	30
TLBO Method	0.0046	0.0019	3.003	5.3998	30

Table 3. CPSS parameter setting with $P_a=P_m-P_e$ input.

	T1	T2	T3	T4	K_{PSS}
COA Method	.0060	1	0	0	3.1250
TLBO Method	0.0058	1	0	0	3.1248

Table 4. SSSC parameter setting.

	KD
COA Method	0.839
TLBO Method	0.852

As revealed by the simulation results shown in Figs.8, 9, 11, and 12, using SSSC alone does not completely remove the SSR effect even with the SSDC extra control [23] so that the system operates under sustained resonance. It is worth noting that the test network employed in [23] is just a single-machine system connected to the infinite bus. Thus, the situation will be even worse in the case of complex systems like the standard one used in this paper. By adding the classic PSS with the speed or the power input, and the simultaneous setting of their parameter and SSSC, the situation gets better and the system becomes more stable with fewer resonance fields, but the resonances are not completely removed.

It was found that better results could be obtained by adopting the method proposed in this paper which involves introducing an MB-PSS and an SSSC into the system while their coefficients are simultaneously set via the TLBO algorithm. With more stable systems, the proposed method may even lead to approximately complete SSR effect removal because the MB-PSS has three working bands at low, medium, and high frequencies. Fig. 13 depicts Bode diagram of the MB-PSS designed using the proposed algorithm.

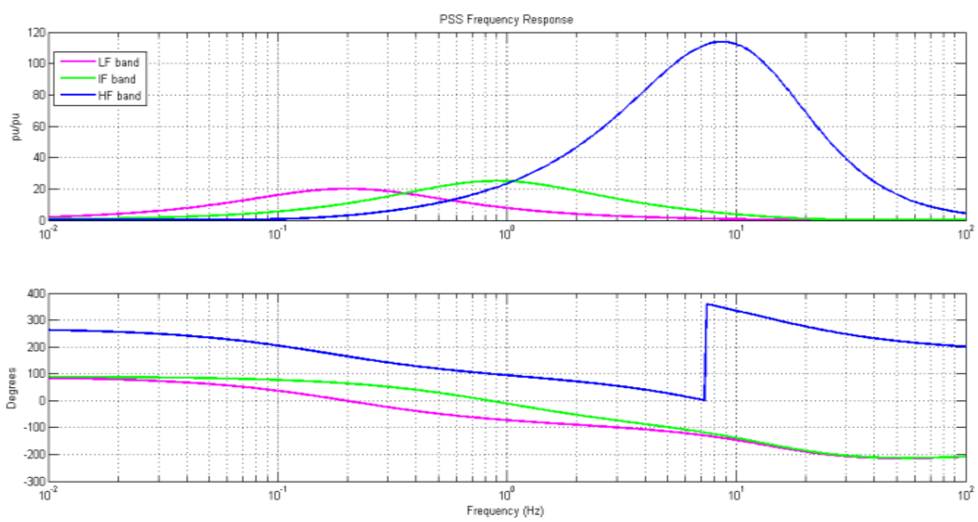

(a)

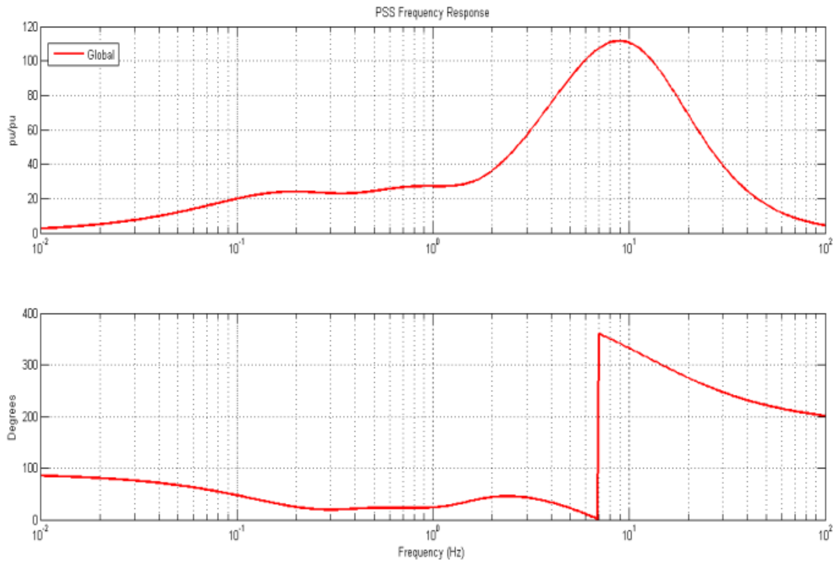

(b)

Fig. 13. MB-PSS diagram: a) the functions of band pass, low pass and high pass bands and b) general MB-PSS function.

According to Fig. 13 (a), each MB-PSS band is responsible for different frequency range. Fig. 13 (b) shows that the MB-PSS generally functions as an intermediate band pass filter as well. Finally, it is seen in Fig. (13) that the central frequency of the MB-PSS is about 50 Hz, which is the main frequency of the network. The system is, therefore, capable of maintaining only the fundamental frequency and eliminates all frequencies due to SSR.

5. CONCLUSION

In this paper, an SSSC was used in combination with an SSDC controller and MB-PSS for SSR damping. The TLBO optimization algorithm was also employed to set the SSDC parameters as well as those of the MB-PSS in order to minimize the resonance field. Results of the simulation confirmed the feasibility of simultaneous application of each of the CPSS stabilizers or MB-PSS with an SSSC equipped with an SSDC controller. The proposed method was also compared with the application of an SSSC alone when dealing with minor and major contingencies in the Benchmark IEEE system. Based on the simulation results, the proposed method was found capable to omit the SSR effect. The proposed power system stabilizer proved to be more efficient and economical than previous systems due to its simplicity and ease of application.

REFERENCES

[1] IEEE Sub Synchronous Resonance Working Group. Terms, "**Definitions and Symbols for Sub Synchronous Oscillations,**" *IEEE Trans. Power App. Syst*, Vol. 104, pp. 1326–1334, 1985.

[2] D. Koteswara Raju, Bhimrao S. Umre, Anjali S. Junghare, B. ChittiBabu, "**Mitigation of Sub Synchronous Resonance with Fractional-order PI based UPFC Controller,**" *Mechanical Systems and Signal Processing*, Vol. 85, pp.698–715, 2017.

[3] F. C. Jusan, S. Jr. Gomes, G. N. Taranto, "**SSR Results obtained with a Dynamic Phasor Model of SVC using Modal Analysis,**" *Electr. Power Energy Syst*, Vol. 32, pp. 571–582, 2010.

[4] R. A. Pahlavani, H. A. Mohammadpour, "**Damping of Sub-Synchronous Resonance and low-Frequency Power Oscillation in a Series-Compensated Transmission Line using Gate-Controlled Series Capacitor,**" *Electr. Power Syst.* Res, Vol. 81, pp. 308–317, 2011.

[5] K. R. Padiyar, N. Prabhu, "**Design and Performance Evaluation of Sub Synchronous Damping Controller with STATCOM,**" *IEEE Trans. Power Deliv*, Vol. 21, pp. 1398–1405, 2006.

[6] M. Alomari, J. G. Zhu, "**Bifurcation Control of Sub Synchronous Resonance using TCSC**," *Commun. Nonlinear Sci. Numer. Simul*, Vol. 16, pp. 2363–2370, 2011.

[7] T. K. C. Sindhu, M. P. Nandakumar, E. P. Cheriyan, "**Adaptive RTRL based Neuro Controller for Damping sub Synchronous Oscillations using TCSC,**" *Eng. Appl. Artif. Intell*, Vol. 24, pp. 60–76, 2011.

[8] S. Panda, "**Multi-objective Evolutionary Algorithm for SSSC-based Controller Design,**" *Electr. Power Syst. Res*, Vol. 79, pp. 937–944, 2009.

[9] G. N. Pillai, A. Ghosh, A. Joshi, "**Torsional Interaction Studies on a Power System Compensated by SSSC and fixed Capacitor,**" *IEEE Trans. Power Deliv*, Vol. 18, pp. 988–993, 2003.

[10] M. El. Moursi, A. M. Sharaf, K. El-Arroudi, "**Optimal Control Schemes for SSSC for Dynamic Series Compensation,**" *Electr Power System Res*, Vol. 78, pp. 646–656, 2008.

[11] J. Chen, T. T. Lie, D. M. Vilathgamuwa, "**Damping of Power System Oscillations using SSSC in Real-Time Implementation,**" *Electr Power Energy Syst*, Vol. 26, pp. 357–364, 2004.

[12] H. Verdejo, D. González, J. Delpiano, C. Becker, "**Tuning of Power System Stabilizers using Multi objective Optimization NSGA II**," *IEEE Latin America Transactions*, Vol. 13, pp. 2653-2660, 2015.

[13] V. S. Vakula, K.R. Sudha, R. Vijayasanthi, "**Particle Swarm Optimization in Fine Tuning of PID Fuzzy Logic Power System Stabilizer,**" *Advances in Computing, Control, and Telecommunication Technologies*, pp. 356-358, 2009.

[14] A. Khodabakhshian, R. Hemmati, M. Moazzami, "**Multi-band Power System Stabilizer Design by using CPCE Algorithm for Multi-Machine Power System,**" *Electric Power Systems Research*, Vol. 101, pp. 36–48, 2013.

[15] Ch. E. Prasad, Sh. Vadhera, "**Fuzzy logic based SSSC as Sub-Synchronous Resonance Damping Controller**," *International Conference on Energy*, pp. 1–4, .2015.

[16] S. Panda, "**Multi-objective Evolutionary Algorithm for SSSC-based Controller Design. Electr,**" *Power Syst. Res*, Vol. 79, pp. 937–944, 2009.

[17] D. Rimorov, I. Kamva, "**Model-based Tuning Approach for Multi-Band Power System Stabilizers PSS4B using an Improved Modal Performance Index,**" *IET Gener. Transm. Distrib*, Vol. 9, pp. 2135–2143, .2015.

[18] S. J. Patel, A. Toshniwal, V. Kheraj, "**A Novel Teaching-Learning Based Optimization Approach for Design of Broad-Band Anti-Reflection Coating,**" *Swarm Evol. Comput*, Vol. 34, pp. 68-74, 2017.

[19] R. V. Rao, V. J. Savsani, D. P. Vakharia, "**Teaching–learning-based Optimization: A Novel Method for Constrained Mechanical Design Optimization Problems,**" *Computer-Aided Design*, Vol. 43, pp. 303-315, 2011.

[20] D. J. Kim, Y. H. Moon, "**SSR Small-Signal Stability Analysis Program of Power Systems and its Application to IEEE Benchmark Systems,**" *Power Tech*, pp. 161–166, 2007.

[21] R. G. Farmer, Chairman, "**Second Benchmark Model for Computer Simulation of Sub Synchronous Resonance,**" *IEEE Power Engineering Review*, Vol. 5, pp. 1057-1066, 1985.

[22] L. D. S. Coelho, "**Tuning of PID Controller for an Automatic Regulator Voltage System using Chaotic Optimization Approach,**" *Chaos Solitons Fractals*. Vol. 39, pp. 1504–1514, 2009.

[23] M. Farahani, "**Damping of Sub Synchronous Oscillations in Power System Using Static Synchronous Series Compensator,**" *IET Gener. Transm. Distrib,* Vol. 6, pp. 539-544, 2012.